

# Quarterly Technical Report

## Selected Energy Epitaxial Deposition and Low Energy Electron Microscopy of AlN, GaN and SiC Thin Films

Supported under Grant #N00014-95-1-0122  
Office of the Chief of Naval Research  
Report for the period 4/1/99-6/30/99

R. F. Davis, H. H. Lamb<sup>†</sup> and I. S. T. Tsong\*,  
E. Bauer\*, R. B. Doak\*, J. L. Edwards\*,  
N. Freed\*, J. Fritsch\*, D. C. Jordan\*, A. McGinnis, A. Pavlovska\*,  
K. E. Schmidt\*, D. J. Smith\*, N. Smith<sup>†</sup> and V. Torres\*

Materials Science and Engineering Department

<sup>†</sup>Chemical Engineering

North Carolina State University

Campus Box 7907

Raleigh, NC 27695-7907

and

\*Department of Physics and Astronomy

Arizona State University

Tempe, AZ 85287-1504

**DISTRIBUTION STATEMENT A**  
Approved for Public Release  
Distribution Unlimited

DTIC QUALITY INSPECTED 2

July, 1999

19991027 109

**REPORT DOCUMENTATION PAGE**

Form Approved  
OMB No. 0704-0188

Public reporting burden for this collection of information is estimated to average 1 hour per response, including the time for reviewing instructions, searching existing data sources, gathering and maintaining the data needed, and completing and reviewing the collection of information. Send comments regarding this burden estimate or any other aspect of this collection of information, including suggestions for reducing this burden to Washington Headquarters Services, Directorate for Information Operations and Reports, 1215 Jefferson Davis Highway, Suite 1204, Arlington, VA 22202-4302, and to the Office of Management and Budget Paperwork Reduction Project (0704-0188), Washington, DC 20503.

1. AGENCY USE ONLY (Leave blank)		2. REPORT DATE July, 1999	3. REPORT TYPE AND DATES COVERED Quarterly: 4/1/99 - 6/30/99	
4. TITLE AND SUBTITLE Selected Energy Epitaxial Deposition and Low Energy Electron Microscopy of AlN, GaN, and SiC Thin Films			5. FUNDING NUMBERS 1213801---01 312 N00179 N66020 4B855	
6. AUTHOR(S) R. F. Davis, H. H. Lamb and I. S. T. Tsong				
7. PERFORMING ORGANIZATION NAME(S) AND ADDRESS(ES) North Carolina State University Hillsborough Street Raleigh, NC 27695			8. PERFORMING ORGANIZATION REPORT NUMBER  N00014-95-1-0122	
9. SPONSORING/MONITORING AGENCY NAMES(S) AND ADDRESS(ES) Sponsoring: ONR, Code 312, 800 N. Quincy, Arlington, VA 22217-5660 Monitoring: Administrative Contracting Officer, Regional Office Atlanta Atlanta Regional Office 100 Alabama Street, Suite 4R15 Atlanta, GA 30303			10. SPONSORING/MONITORING AGENCY REPORT NUMBER	
11. SUPPLEMENTARY NOTES				
12a. DISTRIBUTION/AVAILABILITY STATEMENT  Approved for Public Release; Distribution Unlimited			12b. DISTRIBUTION CODE	
13. ABSTRACT (Maximum 200 words) The homoepitaxial growth of GaN(0001) layers was studied <i>in situ</i> and in real time using the low-energy electron microscope and <i>ex situ</i> using atomic force microscopy and transmission electron microscopy. The growth was conducted on substrates of GaN(0001) deposited on 6H-SiC(0001) by organometallic vapor phase epitaxy. Two growth techniques were employed: one with N-atoms supplied by an RF plasma source and the other with NH <sub>3</sub> molecules seeded in a He supersonic beam. The Ga flux was supplied by an evaporative cell in both cases. Under Ga-rich conditions, non-faceted homoepitaxial layers were achieved on Ga precovered substrate surfaces for both growth methods at 665°C, but the growth morphologies were different. Growing GaN via gas source molecular beam epitaxy (GSMBE), where both the NH <sub>3</sub> and Ga fluxes are known, can establish a correlation between surface morphology and the III/V ratio. The surface morphology is dependent on the III/V ratio and the film growth rate. Under N-stable conditions, increasing the Ga flux (higher III/V ratio) roughens the films until whiskers are formed. Under Ga-stable conditions, increasing the III/V ratio by reducing the ammonia flux yields smoother films, but the growth rate rapidly approaches to zero. Films containing flat hexagonal islands are produced in this limiting case. The III/V ratio does influence the growth morphology, but as reported in this paper, the III/V ratio in itself is not meaningful unless the Ga flux is specified.				
14. SUBJECT TERMS GaN, homoepitaxial growth, low-energy electron microscope, LEEM, seeded-beam supersonic jet, flux ratios, screw dislocations, NH <sub>3</sub> -seeded supersonic molecular beam, atomic force microscopy, growth rate, kinetic energy, surface morphology, cleaning			15. NUMBER OF PAGES 19	
			16. PRICE CODE	
17. SECURITY CLASSIFICATION OF REPORT UNCLAS	18. SECURITY CLASSIFICATION OF THIS PAGE UNCLAS	19. SECURITY CLASSIFICATION OF ABSTRACT UNCLAS	20. LIMITATION OF ABSTRACT SAR	

## I. Introduction

The realized and potential electronic applications of AlN, GaN and SiC are well known. Moreover, a continuous range of solid solutions and pseudomorphic heterostructures of controlled periodicities and tunable band gaps from 2.3 eV (3C-SiC) to 6.3 eV (AlN) have been produced at North Carolina State University (NCSU) and elsewhere in the GaN-AlN and AlN-SiC systems. The wide band gaps of these materials and their strong atomic bonding have allowed the fabrication of high-power, high-frequency and high-temperature devices. However, the high vapor pressures of N and Si in the nitrides and SiC, respectively, force the use of low deposition temperatures with resultant inefficient chemisorption and reduced surface diffusion rates. The use of these low temperatures also increases the probability of the uncontrolled introduction of impurities as well as point, line and planar defects which are likely to be electrically active. An effective method must be found to routinely produce intrinsic epitaxial films of AlN, GaN and SiC having low defect densities.

Recently, Ceyer [1, 2] has demonstrated that the barrier to dissociative chemisorption of a reactant upon collision with a surface can be overcome by the translational energy of the incident molecule. Ceyer's explanation for this process is based upon a potential energy diagram (Fig. 1) similar to that given by classical transition-state theory (or activated-complex theory) in chemical kinetics. The dotted and dashed lines in Fig. 1 show, respectively, the potential wells for molecular physisorption and dissociative chemisorption onto the surface. In general, there will be an energy barrier to overcome for the atoms of the physisorbed molecule to dissociate and chemically bond to the surface. Depending upon the equilibrium positions and well depths of the physisorbed and chemisorbed states, the energy of the transition state  $E^*$  can be less than zero or greater than zero. In the former case, the reaction proceeds spontaneously. In the latter case, the molecule will never proceed from the physisorbed state (the precursor state) to the chemisorbed state unless an additional source of energy can be drawn upon to surmount the barrier. This energy can only come from either (1) the thermal energy of the surface, (2) stored internal energy (rotational and vibrational) of the molecule, or (3) the incident translational kinetic energy of the molecule. Conversion of translational kinetic energy into the required potential energy is the most efficient of these processes. Moreover, by adjusting the kinetic energy,  $E_i$ , of the incoming molecule, it is possible to turn off the reaction ( $E_i < E^*$ ), to tailor the reaction to just proceed ( $E_i = E^*$ ), or to set the amount of excess energy to be released ( $E_i > E^*$ ). The thrust of the present research is to employ these attributes of the beam translational energy to tune the reaction chemistry for wide band gap semiconductor epitaxial growth.

The transition state,  $E^*$ , is essentially the activation energy for dissociation and chemisorption of the incident molecules. Its exact magnitude is unknown, but is most certainly

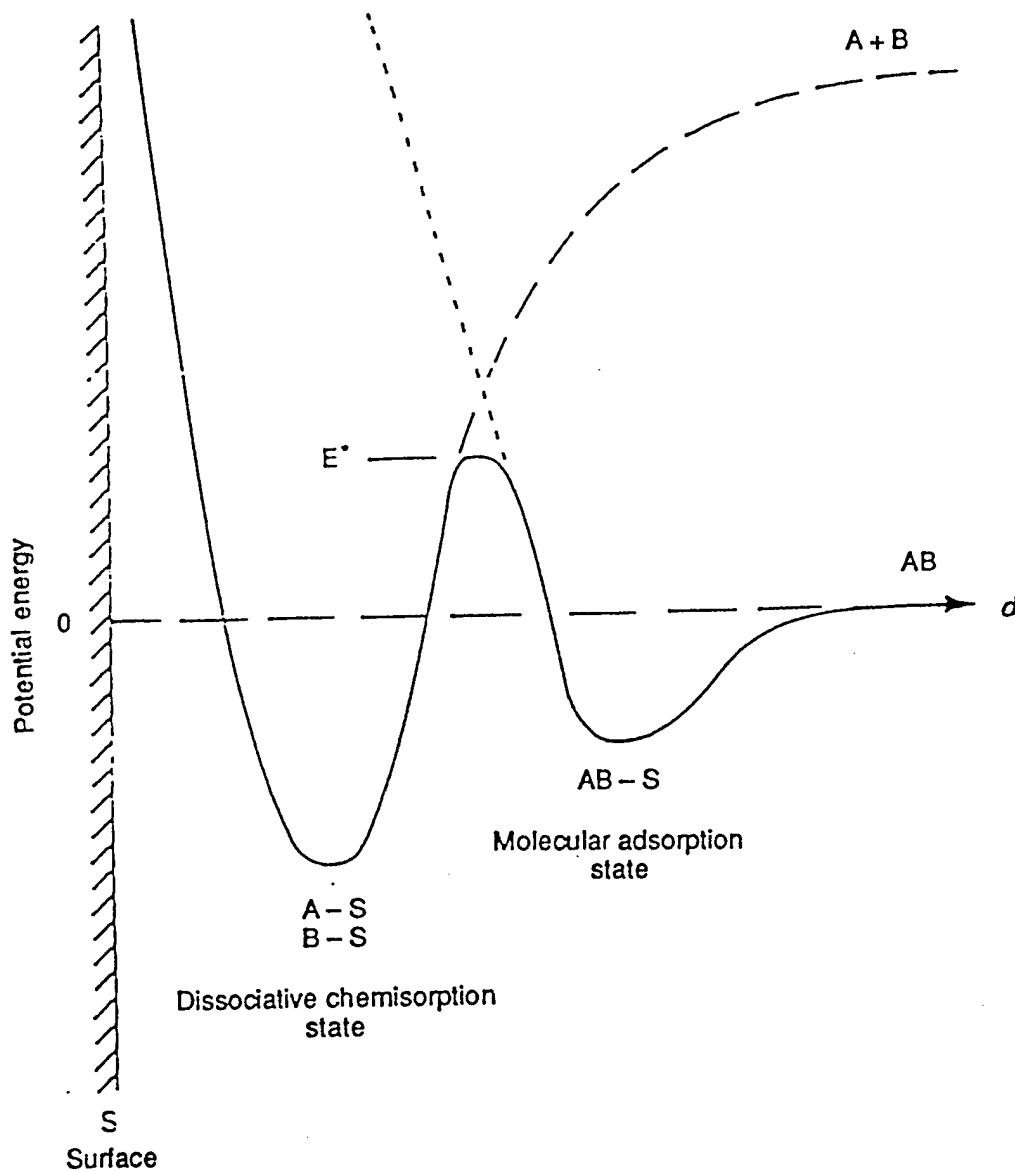


Figure 1. Schematic potential energy diagram of an activated surface reaction involving a molecularly physisorbed precursor state [from Ref. 1].

lower than the dissociation energy of the free molecule. It does not necessarily follow, however, that any kinetic energy above  $E^*$  will promote high-quality epitaxial growth of GaN. One must take into consideration another energy threshold,  $E_d$ , beyond which the kinetic energy of the incident flux will cause damage to the epitaxial film being synthesized. A typical  $E_d$  threshold value is approximately five times the band gap of the crystal and in the case of GaN,  $E_d \approx 18$  eV.

From the above consideration, it is clear that the key to high quality epitaxial growth is to be able to tune the energy of the incoming flux species over a range of energies defined by the window between  $E^*$  and  $E_d$ . Since the window is quite restrictive, i.e. 1-20 eV, it is essential that the energy spread of the flux species must be small, i.e. the flux species should ideally be

monoenergetic. To this end, we employ selected energy epitaxial deposition (SEED) systems for the growth of AlN, GaN and SiC wide band gap semiconductors. The SEED systems are of two types: (1) a seeded-beam supersonic free-jet (SSJ) and (2) a dual ion-beam Colutron. Both these SEED systems have the desirable property of a narrow energy spread of  $\leq 1$  eV.

Epitaxial growth using the seeded-beam SSJ involves a close collaboration between investigators at NCSU and Arizona State University (ASU). At ASU, the SSJ is interfaced directly into a low-energy electron microscope (LEEM) for the conduct of *in situ* studies of the nucleation and growth of epitaxial layers; while at NCSU, the SSJ systems are used to grow device-quality AlN, GaN and SiC for real applications. Exchanges in personnel (students) and information between the two groups ensures the achievement of desired results. The additional thin film growth experiments using dual-beam colutrons and the theoretical studies referred to in this report are primarily conducted at ASU.

The research conducted in this reporting period and described in the following sections has been concerned with (1) the homoepitaxial growth of GaN(0001) layers studied *in situ* and in real time using the low-energy electron microscope and *ex situ* using atomic force microscopy and transmission electron microscopy and 2) homoepitaxial growth of GaN thin films employing MOCVD-grown GaN/SiC substrates. The following individual sections detail the procedures, results, discussions of these results, conclusions and plans for future research. Each subsection is self-contained with its own figures, tables and references.

1. S. T. Ceyer, Langmuir 6, 82 (1990).
2. S. T. Ceyer, Science 249, 133 (1990).

## II. Homoepitaxial GaN Layers Studied by Low-energy Electron Microscopy, Atomic Force Microscopy and Transmission Electron Microscopy

A. Pavlovska, V.M. Torres, J.L. Edwards, E. Bauer, D.J. Smith, R.B. Doak and I.S.T. Tsong  
Department of Physics and Astronomy, Arizona State University,  
Tempe, AZ 85287-1504, USA

D.B. Thomson and R.F. Davis  
Department of Materials Science and Engineering, North Carolina State University,  
Raleigh, NC 27695-7907, USA

The homoepitaxial growth of GaN(0001) layers was studied *in situ* and in real time using the low-energy electron microscope and *ex situ* using atomic force microscopy and transmission electron microscopy. The growth was conducted on substrates of GaN(0001) deposited on 6H-SiC(0001) by organometallic vapor phase epitaxy. Two growth techniques were employed: one with N-atoms supplied by an RF plasma source and the other with NH<sub>3</sub> molecules seeded in a He supersonic beam. The Ga flux was supplied by an evaporative cell in both cases. Under Ga-rich conditions, non-faceted homoepitaxial layers were achieved on Ga precovered substrate surfaces for both growth methods at 665°C, but the growth morphologies were different.

## A. Introduction

In order to achieve an understanding of the effect of growth parameters (e.g. substrate morphology, substrate temperature and flux ratio) on the morphology and structure of GaN films, it is useful to conduct homoepitaxial experiments to eliminate the influence of different substrate materials such as sapphire, SiC and GaAs. Moreover, lattice mismatch induced film stress is not a factor in homoepitaxy.

In this report, we describe *in situ* real-time observations of GaN homoepitaxy using a low-energy electron microscope (LEEM) [1], as well as *ex situ* examination of the GaN homoepitaxial layers by atomic force microscopy (AFM) and by cross-sectional transmission electron microscopy (TEM). Two molecular beam epitaxy (MBE) growth methods were employed, one using  $\text{NH}_3$  molecules seeded into a beam of He atoms from a supersonic jet (SSJ) source and the other using N-atoms from an EPI radio frequency (RF) source. In both cases, the Ga flux was supplied by a conventional Ga effusion cell.

## B. Experimental Procedure

The experimental configuration for conducting LEEM observations of GaN growth by SSJ has been described previously [2]. Typical flux rates were  $(1-10)\times 10^{13} \text{ cm}^{-2}\text{s}^{-1}$  for Ga from an evaporative cell and  $(0.3-3)\times 10^{13} \text{ cm}^{-2}\text{s}^{-1}$  for  $\text{NH}_3$  from the SSJ. The base pressure in the LEEM was  $\sim 1\times 10^{-10}$  torr, which increased to  $3\times 10^{-8}$  torr when the SSJ was in operation. When the N-atom RF plasma source was in use, the pressure in the LEEM rose to  $\sim 1\times 10^{-5}$  torr. The N-atom flux was  $\sim 0.5\times 10^{13} \text{ cm}^{-2}\text{s}^{-1}$  with the RF power at 200 W. The details of calibration of fluxes have been given previously [2].

The GaN(0001) substrates were 1.4  $\mu\text{m}$  thick films grown by organometallic vapor phase epitaxy (OMVPE) on 0.1  $\mu\text{m}$  thick AlN buffer layers on 6H-SiC(0001) mounted on a rotating susceptor [3]. The substrate was cleaned in the LEEM by exposure to a flux of N-atoms from the RF plasma source for 10–15 min at  $\sim 675^\circ\text{C}$ . After the cleaning procedure, the GaN substrate surface generally displayed a  $(\sqrt{3} \times \sqrt{3})$  LEED pattern. Additional treatment by Ga deposition on the substrate at 600–730°C frequently resulted in a (2×2) LEED pattern prior to the homoepitaxy experiments. Bright-field imaging was conducted throughout with the LEEM, i.e. the (00) LEED beam was selected for imaging. In the two examples shown here, the growth rate of the GaN layer determined by cross-sectional TEM was  $\sim 0.5$  nm per hour using the SSJ and  $\sim 10$  nm per hour with the N-atom RF plasma source.

## C. Results and Discussion

The frame-captured LEEM images of GaN homoepitaxial growth at  $665^\circ\text{C}$  with the SSJ are shown in Fig. 1. The Ga flux was  $3.0\times 10^{13} \text{ cm}^{-2}\text{s}^{-1}$  and the  $\text{NH}_3$  flux was  $0.4\times 10^{13} \text{ cm}^{-2}\text{s}^{-1}$ , giving a Ga/ $\text{NH}_3$  flux ratio of  $\sim 8$ . After 30 min of deposition, the surface appeared grainy in frame (b) and the original meandering step structure of the substrate in frame (a) was

completely masked by the graininess. The meandering steps began to reemerge in frame (c), after 70 min of deposition. The step structure was completely restored and sharpened after further deposition as shown in frame (d) taken after 210 min. Deposition was continued for 3.5 more hours, but did not produce significant changes in the surface morphology. The initial LEED pattern of the substrate surface was  $(\sqrt{3} \times \sqrt{3})$ , changing to  $(2 \times 2)$  after 13 min of deposition, and finally to  $(1 \times 1)$  after 57 min. The  $(1 \times 1)$  pattern remained throughout the next 6 hours of growth and no facet spots appeared in the LEED pattern. The LEEM/LEED results thus indicate  $(0001)$  basal plane growth of the GaN homoepitaxial layer.

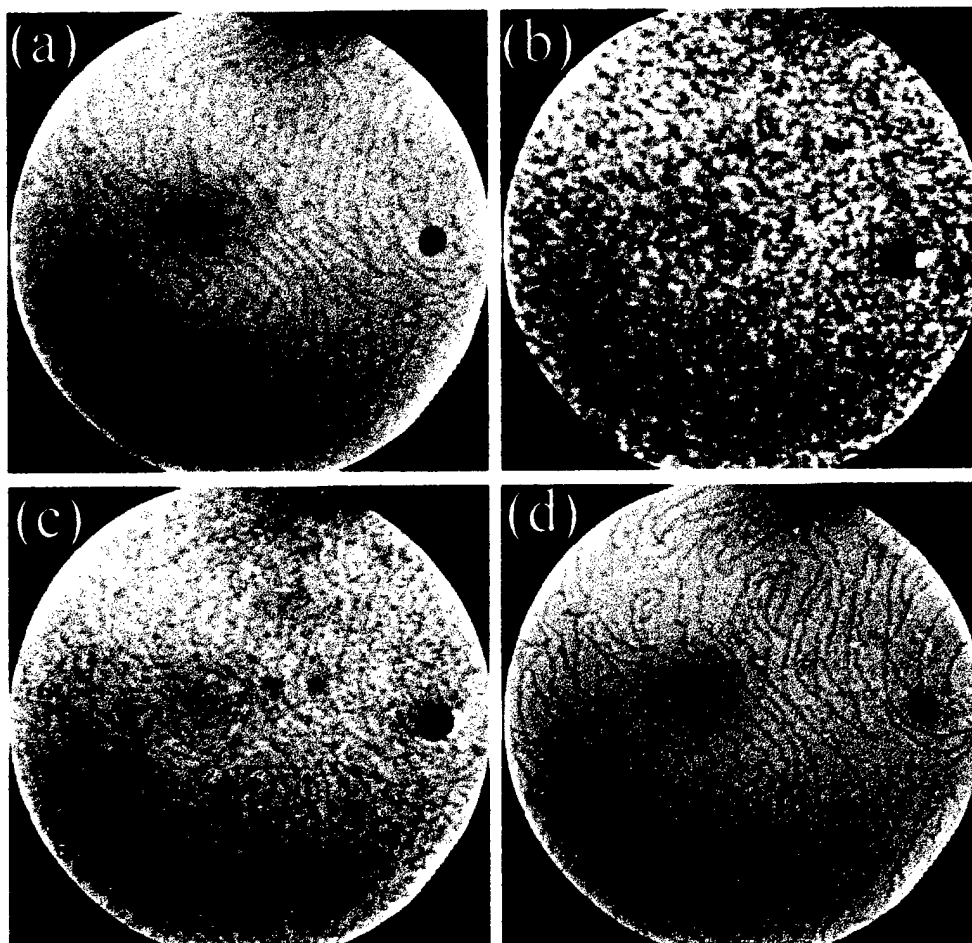


Figure 1. Frame-captured LEEM video images of SSJ homoepitaxial growth of GaN at 665°C on an OMVPE GaN(0001) substrate. (a) Initial  $(\sqrt{3} \times \sqrt{3})$  substrate surface; (b) after 30 min of deposition; (c) after 70 min; and (d) after 210 min. Ga/NH<sub>3</sub> flux ratio ~8. Individual fluxes are given in the text. Electron energy 10.8 eV. Field of view 4.8  $\mu\text{m}$ .

Our *in situ* real-time LEEM/LEED observations of GaN homoepitaxy can be interpreted by the model of quasi-two-dimensional island growth proposed by Headrick *et al.* [4] in their real-time x-ray scattering experiments on the nucleation kinetics of cubic GaN on  $\beta$ -SiC(001). Frame (b) of Fig. 1 represents the initial growth of islands large enough to be resolved by the LEEM. The lateral growth of these islands led to a continuous layer. Once this layer was formed, the meandering steps in frame (d) resumed the sharper appearance visible in frame (a). No further changes could be observed with LEEM after several more hours of deposition and the grainy appearance in frames (b) and (c) was never repeated. This could be due to formation of islands below the resolution limit ( $\sim 10$  nm) of our LEEM prior to coalescence. The initial nucleation, frame (b), occurred on a chemically modified OMVPE GaN(0001) substrate. The completed homoepitaxial GaN(0001) layer in frame (d) was of a different quality because it was grown under UHV, which led to different nucleation conditions. An identical growth sequence was observed within a shorter time period when the individual flux rates were doubled, while keeping the same Ga/NH<sub>3</sub> flux ratio.

A different growth morphology was observed in the second example in which the N-atom RF plasma source was used. In this experiment, the growth temperature was 665°C, the Ga flux was  $\sim 4 \times 10^{13}$  cm<sup>-2</sup> s<sup>-1</sup> and the N-atom flux was  $\sim 0.5 \times 10^{13}$  cm<sup>-2</sup> s<sup>-1</sup>. Under these growth parameters, spiral growth was observed, as shown in the AFM image of Fig. 2(a). Such spiral growth has been observed by Tarsa *et al.* [5] in GaN homoepitaxy using an N-atom RF plasma source under Ga-rich growth conditions. Similar spiral growth was also reported in OMVPE growth of InGaN on a GaN-on-sapphire substrate by Keller *et al.* [6]. Interestingly, many small pits were present on the spiral growth surface in Fig. 2(a). The density of the spirals is  $\sim 5 \times 10^8$  cm<sup>-2</sup> and the pit density is  $\sim 3 \times 10^9$  cm<sup>-2</sup>. These numbers are similar to those reported by Tarsa *et al.* [5] for their homoepitaxial GaN surface. The growth of spiral mounds has also been observed in other systems, such as InP/InP [7], GaAs/GaAs [8] and GaSb/GaAs [9,10]. The spirals are generally attributed to step-flow growth at the surface termination of screw dislocations. Thus, the number density of spirals probably reflects the density of terminations of the threading dislocations with screw components at the OMVPE substrate surface.

The surface pits have a lateral size distribution ranging from 30 to 60 nm, with some showing a hexagonal symmetry in AFM images of higher magnification, as shown in Fig. 2(b). The depths of these pits range from 5 to 9 nm as measured by cross-sectional TEM images such as that shown in Fig. 3. Their locations on the surface appear to be random. These pits are, thus, not associated with hollow-core screw dislocations found in OMVPE GaN epilayers [11]. However, their sizes are similar to the inverted hexagonal pyramidal defects with (10 $\bar{1}$ 1) facets observed in InGaN/GaN multiple quantum wells [12,13]. Northrup *et al.* [14] propose that the segregation of In on the (10 $\bar{1}$ 1) facets lower the surface energy, thereby

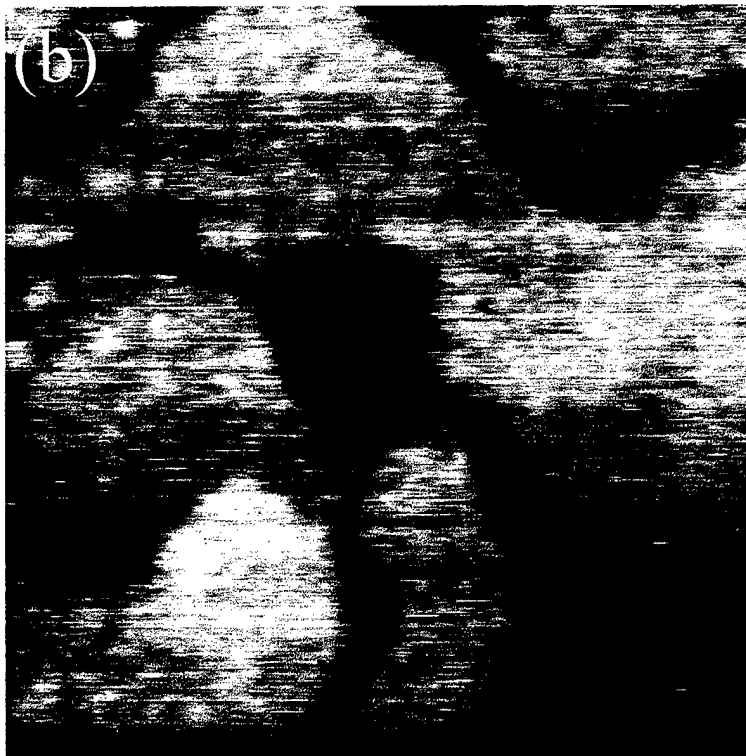
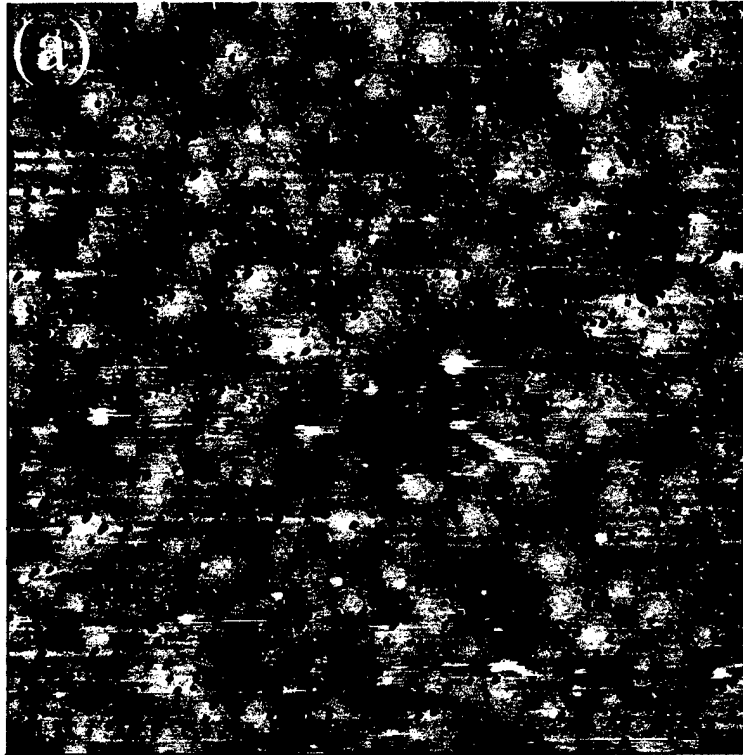


Figure 2. AFM images of homoepitaxial GaN layer grown with the N-atom RF plasma source showing growth of spirals and surface pits. Ga/N flux ratio  $\sim 8$ . Growth temperature  $665^{\circ}\text{C}$ . a) scan area  $5\ \mu\text{m} \times 5\ \mu\text{m}$ , b) scan area  $250\ \text{nm} \times 250\ \text{nm}$ .

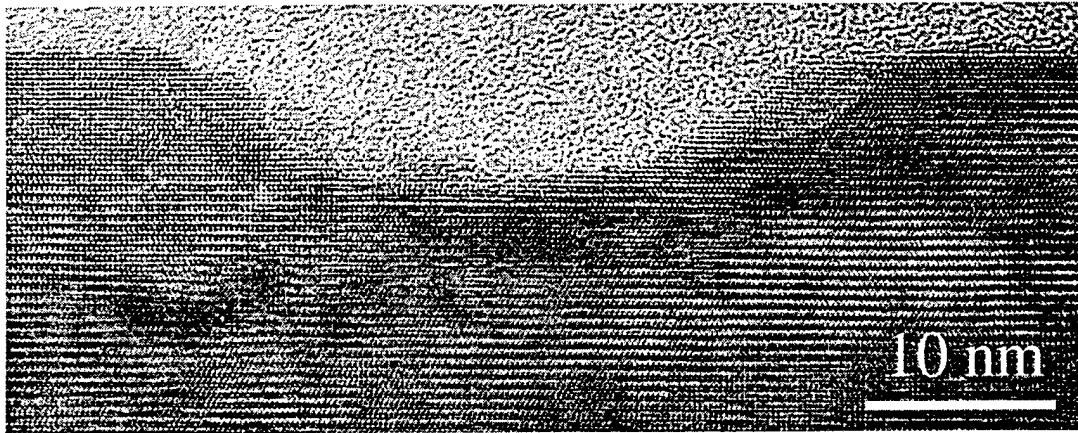


Figure 3 Cross-sectional TEM image of a surface pit on the GaN homoepitaxial layer shown in Fig. 2.

leading to their large sizes. In the surface pits observed in Figs. 2 and 3, there were no facets within the pits and there was no indium acting as impurity segregation in our growth process. Both bright-field and dark-field TEM images clearly establish that the surface pits are not related to threading dislocations. It is possible that under our Ga-rich growth conditions, small droplets of liquid Ga on the surface hindered the growth of GaN in the area covered by the droplet because it was undersaturated with respect to N-atoms at the growth temperature. As growth continued around the droplet, eventually a pit was formed.

#### D. Conclusions

We have shown that under Ga-rich growth conditions, (0001) basal plane GaN homoepitaxial layers can be achieved in two MBE growth methods, one with an  $\text{NH}_3$  seeded-beam SSJ source and the other with an N-atom RF plasma source. Two examples have been given, one with nucleation of small two-dimensional islands and the other with spiral growth.

#### E. Acknowledgements

We thank U. Knipping for technical assistance and I.S.T.T. thanks S. Mahajan for useful discussions. This work was supported by Office of Naval Research grant N00014-95-1-0122 (Colin Wood, Technical Monitor) and National Science Foundation MRSEC grant DMR-9632635.

#### F. References

1. E. Bauer, Rep. Prog. Phys. **57**, 895 (1994).
2. A. Pavlovska, E. Bauer, V.M. Torres, J.L. Edwards, R.B. Doak, I.S.T. Tsong, V. Ramachandran and R.M. Feenstra, J. Cryst. Growth **189/190**, 310 (1998).
3. T.W. Weeks, Jr., M.D. Bremser, K.S. Ailey, E.P. Carlson, W.G. Perry and R.F. Davis, Appl. Phys. Lett. **67**, 401 (1995).
4. R.L. Headrick, S. Kycia, Y.K. Park, A.R. Woll and J.D. Brock, Phys. Rev. B **54**, 14686 (1996).

5. E.J. Tarsa, B. Heying, X.H. Wu, P. Fini, S.P. DenBaars and J.S. Speck, *J. Appl. Phys.* **82**, 5472 (1997).
6. S. Keller, U.K. Mishra, S.P. DenBaars and W. Seifert, *Jpn. J. Appl. Phys.* **37**, L431 (1998).
7. C.C. Hsu, J.B. Xu and I.H. Wilson, *Appl. Phys Lett.* **65**, 1394 (1994).
8. C.C. Hsu, J.B. Xu, I. H. Wilson, T.G. Anderson and J.V. Thordson, *Appl. Phys. Lett.* **65**, 1552 (1994).
9. B. Brar and D. Leonard, *Appl. Phys. Lett.* **66**, 463 (1995).
10. S.J. Brown, M.P. Grimshaw, D.A. Ritchie and G.A.C. Jones, *Appl. Phys. Lett.* **69**, 1468 (1996).
11. W. Qian, G.S. Rohrer, M. Skowrouski, K. Doverspike, L.B. Rowland and D.K. Gaskill, *Appl. Phys. Lett.* **67**, 2284 (1995).
12. Y. Chen, T. Takeuchi, H. Amano, I. Akasaki, N. Yamada, Y. Kaneko and S.Y. Wang, *Appl. Phys. Lett.* **72**, 710 (1998).
13. X.H. Wu, C.R. Blass, A. Abare, M. Mack, S. Keller, P.M. Petroff, S.P. DenBaars, J.S. Speck and S.J. Rosner, *Appl. Phys Lett.* **72**, 692 (1998).
14. J.E. Northrup, L.T. Romano and J. Neugebauer, *Appl. Phys. Lett.* **74**, 2319 (1999).

### III. Surface Morphology of GaN Grown by Gas Source Molecular Beam Epitaxy (GSMBE)

#### A. Introduction

Selected energy epitaxy (SEE) using  $\text{NH}_3$ -seeded supersonic beams is an alternative to plasma-source molecular beam epitaxy (PMBE) for low-temperature growth of III-nitride semiconductors. Homoepitaxial growth of GaN thin films employing MOCVD-grown GaN/SiC substrates is the research focus. As discussed in the December 1998 report, changes in the V/III ratio can produce a transition between three-dimensional (3D) and two-dimensional epitaxial growth. In recent literature, a high III/V ratio (Ga-stable growth) favored 2D growth while a low III/V ratio (N-stable growth) favored 3D growth. Growing GaN via gas source molecular beam epitaxy (GSMBE), where both the  $\text{NH}_3$  and Ga fluxes are known, can establish a correlation between surface morphology and the III/V ratio. After establishing the correlation, GaN will be grown using SEE. The morphology of SEE-grown GaN will be compared to samples grown by GSMBE in order that the SEE process parameters may be optimized. The comparison will also determine if SEE (beam seeded with  $\text{NH}_3$ ) grown GaN offers advantages over GSMBE ( $\text{NH}_3$  leak valve) grown GaN.

#### B. Experimental Procedure

The substrates were 1–2  $\mu\text{m}$  thick GaN films grown by MOCVD at  $1050^\circ\text{C}$  on 6H-SiC using a 0.1  $\mu\text{m}$  AlN buffer layer. Wafers of GaN/AlN/SiC were obtained from the Davis group. The surface morphology of these substrates is shown in Fig. 1. A tungsten film ( $\sim 0.1 \mu\text{m}$ ) was deposited by RF sputtering on SiC face, and approximately  $1 \times 1 \text{ cm}^2$  samples were cut using a diamond saw. Samples were degreased using trichloroethylene (TCE) prior to mounting on a Mo sample holder. Surface morphologies were characterized using an AFM (DI

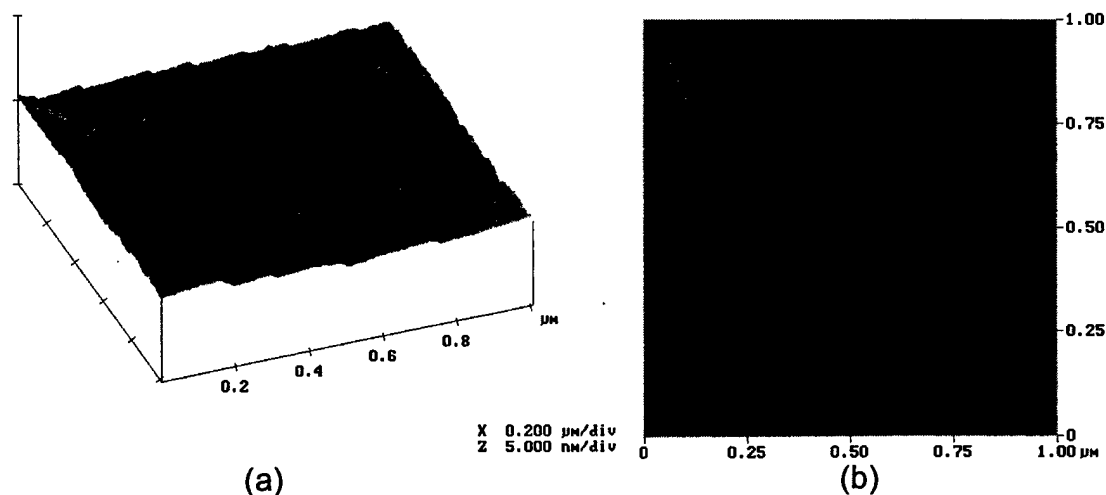


Figure 1. AFM image of surface morphology of GaN grown by MOCVD. The RMS roughness of the sample is 0.16 nm.

Dimension 3000) and a SEM (JEOL JSM-6400F). The thickness of films (step height between the area masked by the pin and film) was measured using profilometer (Tencor alpha-step 200).

The SEE growth system has been described in detail in previous reports. In the first set of experiments, the ammonia partial pressure was held constant while the Ga K-cell temperature was varied. In the second set of experiments, the Ga K-cell temperature was held constant while the partial pressure of ammonia was varied. All depositions were carried out at 750°C for two hours.

### C. Results and Discussion

Films were first grown for two hours at 750°C with a constant ammonia partial pressure of  $1.5 \times 10^{-5}$  torr. The background vacuum of the deposition chamber was raised from  $1 \times 10^{-9}$  to  $1.5 \times 10^{-5}$  torr by introducing  $\text{NH}_3$  via a leak valve. Films were grown with Ga K-cell temperatures of 980°C, 1000°C, 1029°C and 1050°C. The surface morphologies of the films are shown in Fig. 2. The higher Ga flux increased the thickness of the films and also increased the roughness of the films. The growth morphology of the samples under increasing III/V ratio is contrary to findings stated in the literature. The higher Ga fluxes produce GaN whiskers with growth rates as high as 1.2  $\mu\text{m/hr}$ . The statistical roughening of the films is due to decreasing mean free path length of Ga adatoms at higher growth rates.

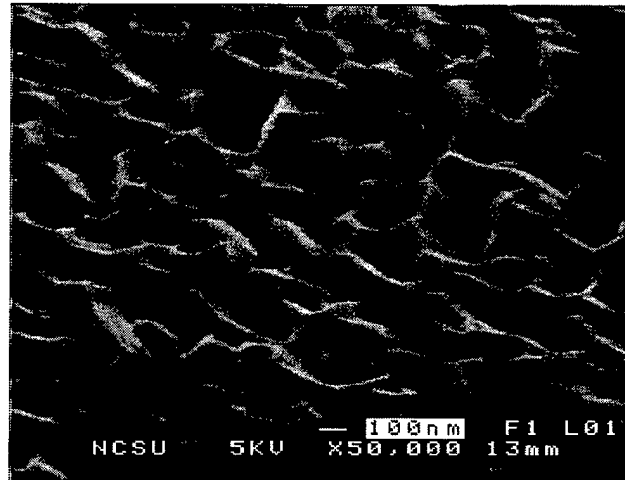
A plot of equivalent GaN flux ( $F_{\text{GaN}}$ ) vs. Ga flux ( $F_{\text{Ga}}$ ) is shown in Figure 3. The following relationship (from last report) was used to calculate Ga flux:

$$\ln(F_{\text{Ga}}) = \frac{1}{2} \cdot \left( 55.29 - \frac{26550}{T} \right) \quad (1)$$

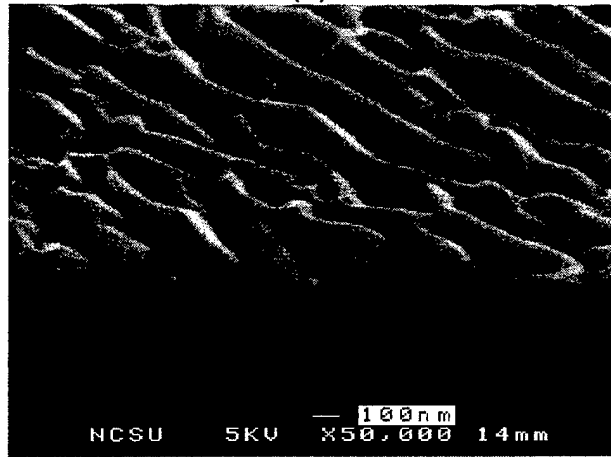
where  $F_{\text{Ga}}$  is the Ga flux in  $\text{cm}^{-2}\text{s}^{-1}$  and  $T$  is the absolute temperature in K. The equivalent GaN flux ( $F_{\text{GaN}}$ ) was calculated using the following relationship:

$$F_{\text{GaN}} = \frac{\rho_{\text{GaN}} \cdot G \cdot N_{\text{Av.}}}{M_{\text{GaN}}} \quad (2)$$

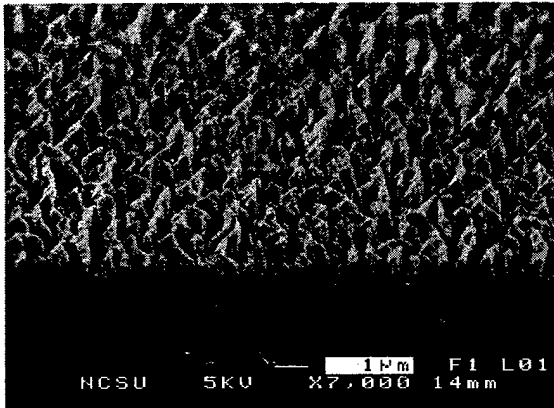
where  $\rho_{\text{GaN}}$  is the GaN density,  $G$  is the growth rate,  $N_{\text{Av.}}$  is the Avogadro's number, and  $M_{\text{GaN}}$  is the molecular weight of GaN. The growth rate varies approximately linearly with Ga flux indicating N-stable growth. As seen in Fig. 2, the samples grown with Ga K-cell temperatures of 1029°C and 1050°C have spaces (voids) between the whiskers. The actual value for  $F_{\text{GaN}}$  is less than the calculated value given that  $\rho_{\text{film}} < \rho_{\text{GaN}}$  since there are spaces between the whiskers.



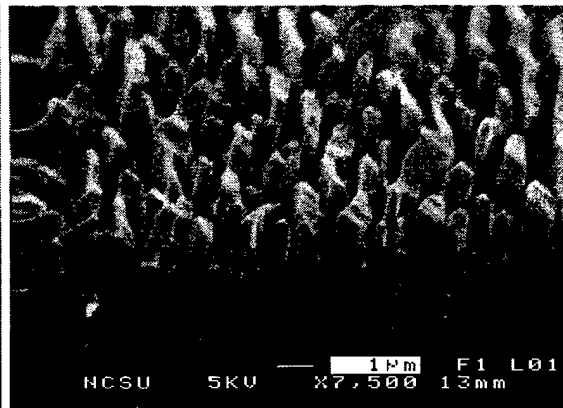
(a)



(b)



(c)



(d)

Figure 2. SEM micrographs of GaN grown by GSMBE at 750°C under  $\text{NH}_3$  partial pressure of  $1.5 \times 10^{-5}$  torr with Ga K-cell temperatures of (a) 980°C, (b) 1000°C, (c) 1029°C and (d) 1050°C. The thickness of the films are (a) 0.55  $\mu\text{m}$ , (b) 0.73  $\mu\text{m}$ , (c) 1.7  $\mu\text{m}$  and (d) 2.4  $\mu\text{m}$ .

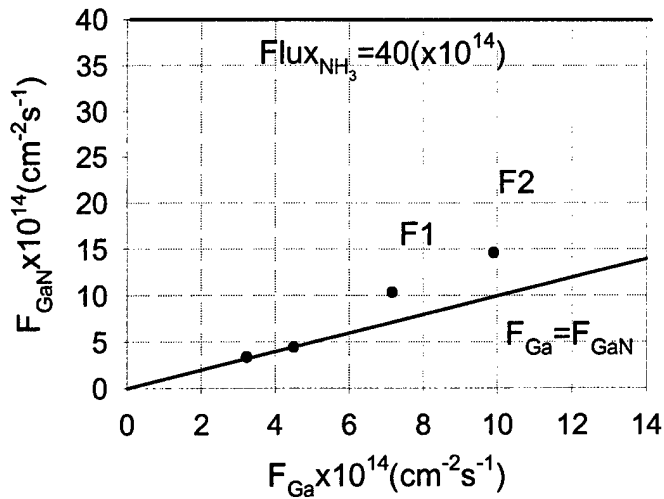


Figure 3. GaN growth kinetics under N-stable conditions for samples grown with Ga K-cell temperature of 980°C, 1000°C, 1029°C and 1050°C. Points F1 and F2 are overestimates of the actual  $F_{\text{GaN}}$  since the density of GaN is used instead of the density of the film. The density of the film is unknown since the volume fractions of the GaN whiskers and of the spaces between them are unknown.

In the next series of experiments, the Ga K-cell temperature was held constant at 1000°C, and the ammonia flux ( $F_{\text{NH}_3}$ ) was varied. All films were grown for 2 hours at 750°C. Table I lists the growth conditions, final thickness and roughness of the films. The AFM images of the films are shown in Figs. 4 and 5.

Table I. Growth Conditions, Final Thickness and Roughness of Films

NH <sub>3</sub> Partial Pressure (torr)	III/V Ratio	Final Film Thickness (μm)	RMS Roughness (nm)
$1.5 \times 10^{-5}$	0.11	0.73	56.5
$7.7 \times 10^{-6}$	0.22	0.77	54.4
$3.8 \times 10^{-6}$	0.44	0.69	22.9
$2.8 \times 10^{-6}$	0.61	0.56	18.1
$1.5 \times 10^{-6}$	1.11	~ 0.1	11.6 (0.7 between hexagonal formations)
$7.7 \times 10^{-7}$	2.21	~ 0.1	5.0 (0.6 between droplets)

As the  $\text{NH}_3$  flux is decreased, films go from a rough 3-D morphology to a flat morphology with flat hexagonal GaN islands and steps (Fig. 4e). At the lowest  $\text{NH}_3$  flux (Fig. 4f), Ga droplets appeared, and the steps disappeared – easily seen in Fig. 5e. There is a relationship between the roughness of the film and its growth rate.

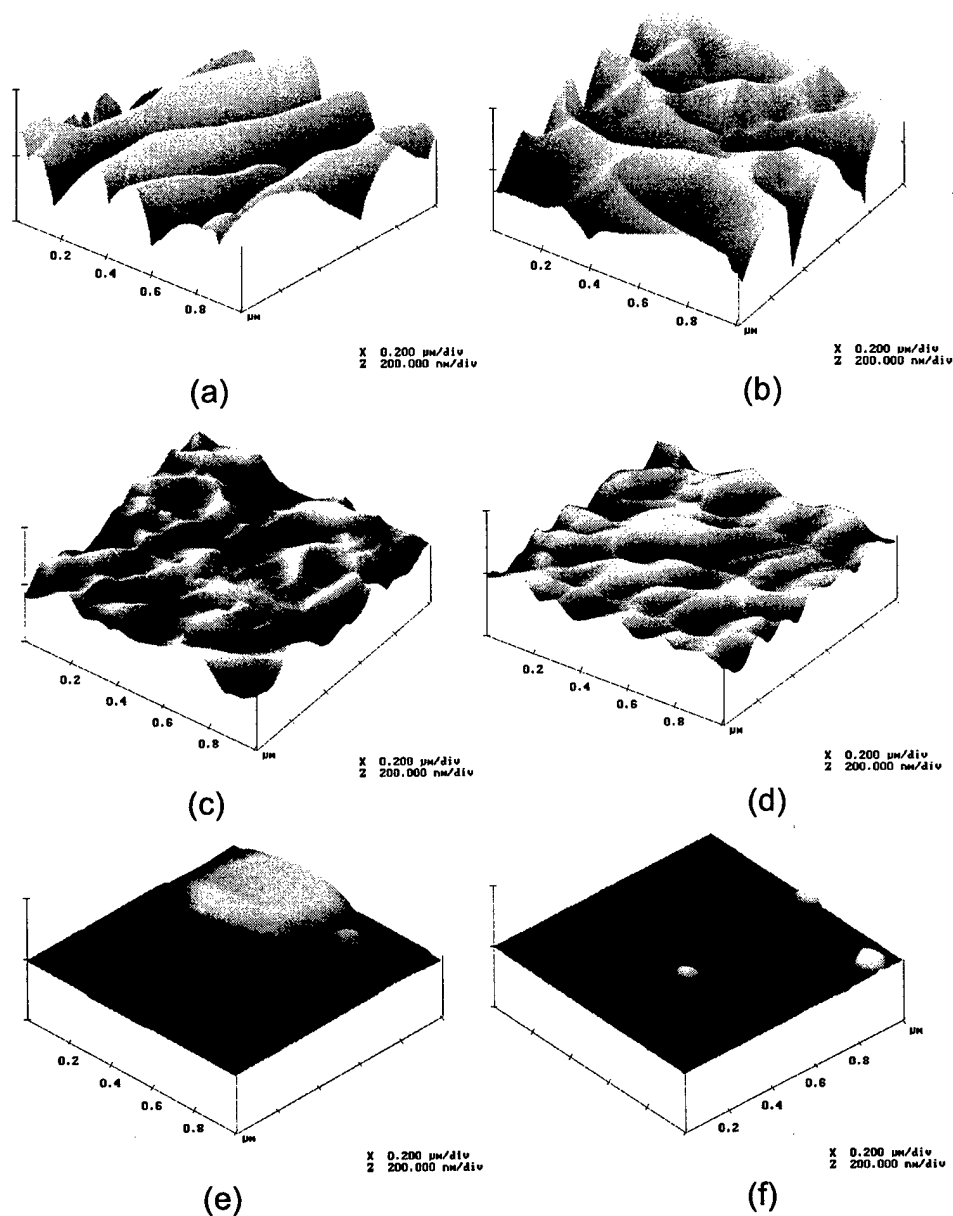


Figure 4.  $(1 \times 1) \mu\text{m}^2$  AFM images of GaN grown by GSMBE with constant Ga K-cell temperature of  $1000^\circ\text{C}$  with  $\text{NH}_3$  partial pressure set at (a)  $1.5 \times 10^{-5}$ , (b)  $7.7 \times 10^{-6}$ , (c)  $3.8 \times 10^{-6}$ , (d)  $2.8 \times 10^{-6}$ , (e)  $1.5 \times 10^{-6}$  and (f)  $7.7 \times 10^{-7}$  torr.

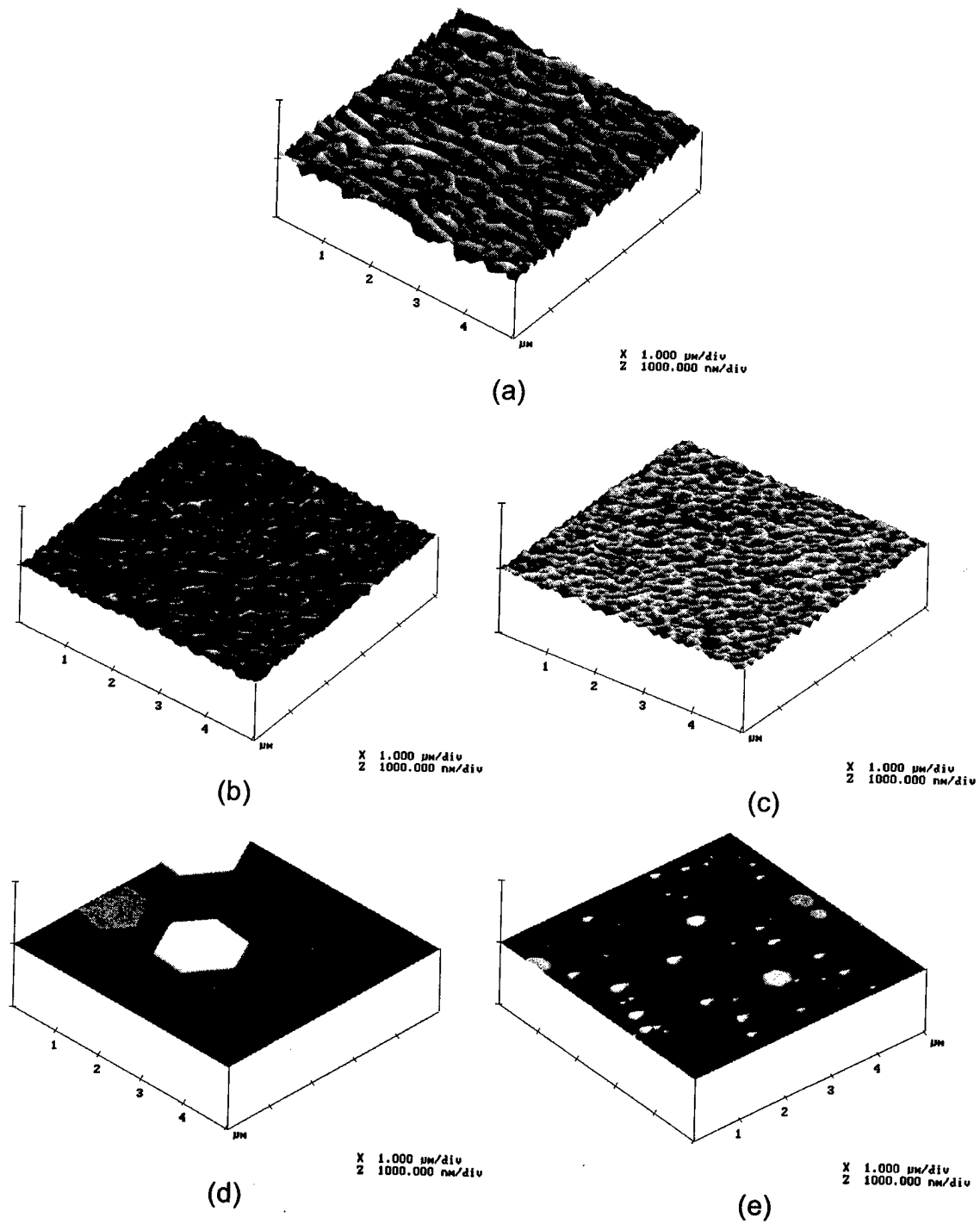


Figure 5.  $(5 \times 5) \mu\text{m}^2$  AFM images of GaN grown by GSMBE with constant Ga K-cell temperature of  $1000^\circ\text{C}$  with  $\text{NH}_3$  partial pressure set at (a)  $7.7 \times 10^{-6}$ , (b)  $3.8 \times 10^{-6}$ , (c)  $2.8 \times 10^{-6}$ , (d)  $1.5 \times 10^{-6}$  and (e)  $7.7 \times 10^{-7}$  torr.

The AFM section analysis (Fig. 6) gives height information on the hexagonal island. The height and width of the hexagonal island is 25 nm and 1.5 μm, respectively. The step height between the hexagonal island is 3.1 nm.

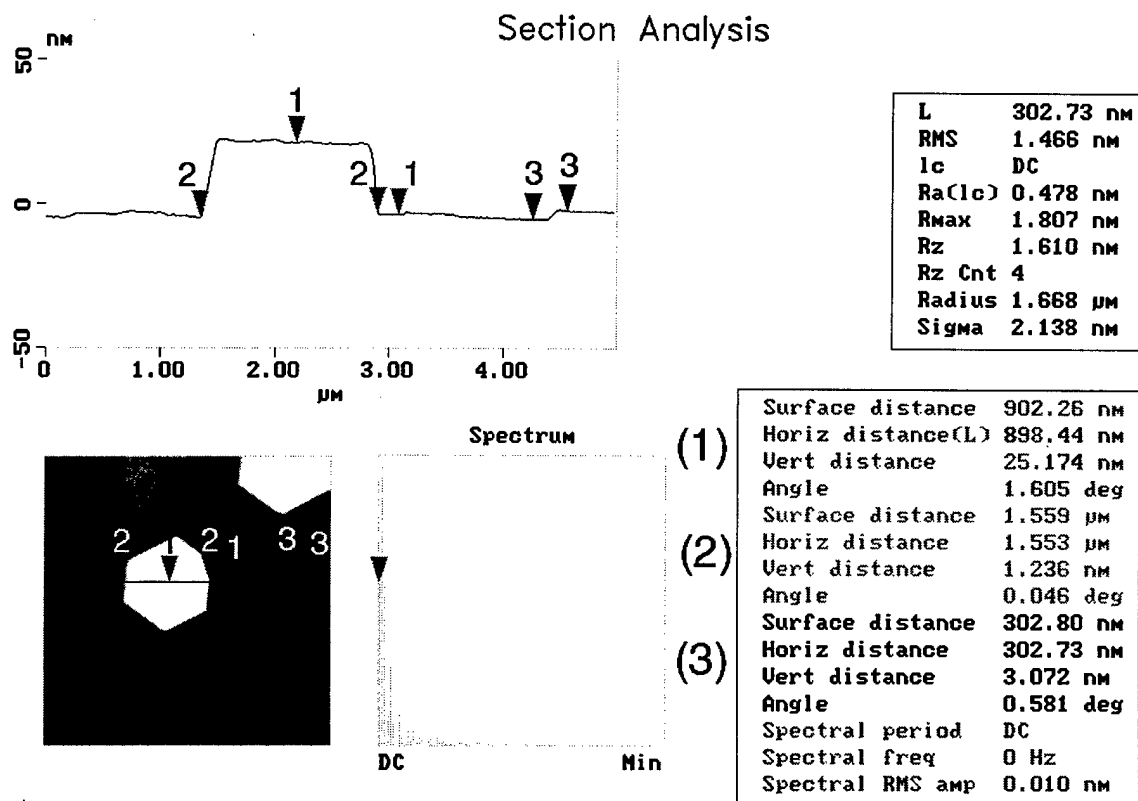


Figure 6. AFM section analysis of GaN grown by GSMBE at  $\text{NH}_3$  partial pressure of  $1.5 \times 10^{-6}$  torr. The height and width of the large hexagonal structure are 25.1 nm and 1.6 μm, respectively. The height of the step between hexagonal island is 3.1 nm.

The GaN growth rate varied with  $\text{NH}_3$  partial pressures as shown in Fig. 7. Equation 2 was used to calculate  $F_{\text{GaN}}$ . The flux for  $\text{NH}_3$  ( $F_{\text{NH}_3}$ ) is given by the following relationship:

$$F_{\text{NH}_3} = \left( \frac{1}{2\pi \cdot M_{\text{NH}_3} \cdot k \cdot T} \right)^{\frac{1}{2}} = \frac{3.51 \times 10^{22} \cdot p_0}{\sqrt{M_{\text{NH}_3} \cdot T}} \quad (3)$$

where  $k$  is the Boltzmann constant,  $T$  is the absolute temperature in K,  $p_0$  is the equilibrium vapor pressure and  $M_{\text{GaN}}$  is the molecular weight of GaN. Figure 7 illustrates that, for partial pressure  $\geq 7.7 \times 10^{-6}$  torr, the thickness of the films did not vary with  $F_{\text{NH}_3}$  suggesting Ga-limited (N-stable) growth. Figure 7 also illustrated that, for  $\text{NH}_3$  partial pressure

$\leq 7.7 \times 10^{-6}$  torr, the thickness of the films did vary with  $F_{\text{NH}_3}$  suggesting  $\text{NH}_3$  limited (Ga-stable) growth conditions. There was some difficulty in measuring the film thickness of samples grown under ammonia partial pressures of  $7.7 \times 10^{-7}$  and  $1.5 \times 10^{-6}$  torr since the films are so thin. The growth morphology of the films under increasing III/V ratio agrees with findings reported in the literature.

In conclusion, the surface morphology is dependent on the III/V ratio and the film growth rate. Under N-stable conditions, increasing the Ga flux (higher III/V ratio) roughens the films until whiskers are formed. Under Ga-stable conditions, increasing the III/V ratio by reducing the ammonia flux yields smoother films, but the growth rate rapidly approaches to zero. Films containing flat hexagonal islands are produced in this limiting case. The III/V ratio does influence the growth morphology, but as reported in this paper, the III/V ratio in itself is not meaningful unless the Ga flux is specified.

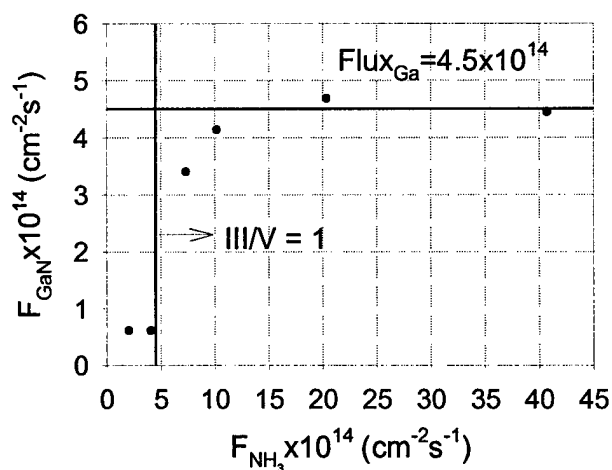


Figure 7.  $\text{NH}_3$  partial pressure  $\geq 7.7 \times 10^{-6}$  torr indicated Ga-limited (N-stable) growth conditions while partial pressure  $\leq 7.7 \times 10^{-6}$  torr indicated  $\text{NH}_3$  limited (Ga-stable) growth conditions. There was some difficulty in measuring differences in thickness for samples with very low growth rate.

#### IV. Distribution List

Dr. Colin Wood Office of Naval Research Electronics Division, Code: 312 Ballston Tower One 800 N. Quincy Street Arlington, Va 22217-5660	3
Administrative Contracting Officer Office of Naval Research Regional Office Atlanta 100 Alabama Street, Suite 4R15 Atlanta, Ga 30303	1
Director, Naval Research Laboratory ATTN: Code 2627 Washington, DC 20375	1
Defense Technical Information Center 8725 John J. Kingman Road, Suite 0944 Ft. Belvoir, VA 22060-6218	2